Supporting Information

Polarity-Dominated Stable N97 Respirators for Airborne Virus Capture Based on Nanofibrous Membranes

Qifei Wang, Yingzhen Wei, Wenbo Li, Xizi Luo, Xinyue Zhang, Jiancheng Di, Guoqing Wang, and Jihong Yu*

anie_202108951_sm_miscellaneous_information.pdf

SUPPORTING INFORMATION

Table of Contents

SUPPORTING INFORMATION

Experimental Procedures

Materials and Methods

Materials

Polyacrylonitrile (PAN, 150,000, 90%) was purchased from the Jilin Chemical Company (China). Dimethylformamide (DMF), hydrazine dihydrochloride were purchased from Beijing Chemical Company (China). 1,4-Dicyanobezene (98%), and 4-cyanobenzoic acid (99%) were purchased from ACROS Organic Company (Belgium). 4-(Trifluoromethoxy)benzonitrile (98%) was purchased from Aladdin Company (China). 4-Fluorophenylacetonitrile (97%) was purchased from ALFA Company (USA). 4-Aminobenzonitrile (98%) was purchased from Innochem company (China). Hydrazine hydrate (80 wt%), and dimethyl sulfoxide (DMSO) were purchased from Tianjin Fuchen Chemical Company (China). Ethylene glycol, nitromethane and formamide were purchased from Beijing Chemical Company (China). The DMEM and fetal bovine serum (FBS, Gibico) were purchased from Invitrogen TM Co., Ltd (USA). The burning incense was purchased from Tongda manufacturing company (China).

Sample preparation

The polyacrylonitrile nanofibrous membrane (PNM) was fabricated via the electrospinning technique based on our previous work. Typically, 1.0 g PAN was mixed with 9.0 g DMF solution containing 0.05 g water, then the mixture was stirred at 50 °C until the solid was completely dissolved. The precursor solution was loaded into the electrospinning system. The aluminum foil (5.0 × 5.0 cm) was used as the collector with electrospinning time and the working distance was kept at 30 min and 15 cm, respectively. Then the as-prepared PNM was subsequently followed by two post modification processes to achieve the alteration of surface terminal groups: (1) the preparation of 4-cyan-Ph-terminated thin-film coated PNM (CTFPNM); (2) the thin-film coatings with other terminal groups were fabricated on the as-prepared CTFPNM. All the experiment details were precisely recorded in our previous work.[1]

We chose multiple N95-grade FFRs for test: (1) Dräger X-plore 1095 (France, GB2626 KN95), (2) MEO (New Zealand, AS/NZS KN95), (3) KINLEED (China, GB2626 KN95), (4) 3Q (China, GB19083 N95) and (5) 3M 8210 (The United State, NOISH N95). All the samples were tested with a flow rate of 5 L/min.

Charging

A 5 cm × 5 cm TFPNM was prepared for the injection of electrostatic charges. The demonstration is shown in Figure 1. The charging distance was kept as 30 mm for 5 min with a charging voltage at 16 kV. A 5-wire charging tip was self-made to inject electrostatic charges onto the membrane and insure the uniform distribution of the charges.

Electrostatic charges measurement

The electrostatic charge quantity was measured by a hand-hold electrostatic fieldmeter (FMX-004, SIMCO, Japan). The tested distance was kept at 2cm. 10 samples were selected from each respirator membrane and 5 points were chosen on each sample to ensure the accuracy.

PM simulation

The PM particulates were simulated by the smoke generated from the burning incense. The smoke PM particulates have a wide range in size from < 300 nm to > 10 µm.[2] The inflow concentration was controlled over 1000 µg/m^3 (PM2.5 number density > 17650 per m^3).

Preparation of virus solutions

In this study, Coxsackie B4 virus (CV-B4) was used as provided by G. Wang, Pathogenic Microbiology Laboratory of Jilin University, China. Each virus solution was prepared by diluting 0.1 ml initial virus solution (CV-B4: $TCID_{50}= 10^7/0.1$ ml) into 50 ml deionized (DI) water. Moreover, all related experiments were performed inside a class II Biosafety Cabinet (BHC-1300IIB2, AIRTEC., China) in a BSL II laboratory.

Filtration efficiency measurement

The filtration efficiency was calculated by comparing the PM/aerosols particulate number detected before and after the filtering for each filtration cycle (for 1 h), and the samples were subsequently tested and followed with a new cycle.The filtration processes were all conducted with an air flow at 5 L/min. 10 samples were selected from each respirator membrane and 5 spots were chosen on each sample to ensure the accuracy.

Cytopathic effect and virus titration tests

HeLa cells were cultured in DMEM supplemented with 10% (v/v) fetal bovine serum (FBS) and penicillin (100 U/ml), streptomycin (100 µg/ml), in a humidified incubator with 5% carbon dioxide at 37 °C. In order to exclude the influence on viruses of aerosolization and experimental condition, especially the room humidity (RH), the viruses for further measurements were all collected after aerosolization with the same experimental condition at 23 °C ± 3 °C, 45 % ± 5 % RH.[3]

The cells with polyhedral morphology were grown in 96-well plates until reaching to 80% confluence. The viral aerosols before or after the filtration were collected by an All-Glass-Impinger (AGI-30) with 20 ml DMEM solution and 100 µl of the solution was added to replace the inoculum, and after 2 h at 37 °C, the viral solution was removed, and the cells were washed three times with DMEM, and then incubated in the DMEM containing 2% FBS for 5 days and then the cultures were observed by light microscope for viral cytopathic

effects (CPE). The cytopathic changes occurred on the HeLa cells finally leading to shrinkage, rounding and a cell release from the monolayer.[4] A serial 10-fold dilution of the viral solution suspension was made and inoculated in eight wells of a 96-well plate at 37 °C, the dilution that causes cytopathology in half of the cultures (the median tissue culture infective dose, $TCID_{50}$/ml) was observed and calculated after Spearman and Kaerber.[5]

Heat treatment

All the samples were placed into a heating oven (SENXIN, DGG-9070B) at 80 °C for 30 min. Every sample was then tested within a filtration cycle for 1 h with NaCl aerosols (0.26 μm medium diameter). After filtering, the samples were replaced into the heating oven to start a new treatment cycle.

Steam treatment

All the samples were placed on the top of a crystallizing dish filled of boiling water for 10 min, and the height between the samples and the water was controlled at 10 cm. The samples were subsequently tested and followed with a new treatment cycle.

75% Alcohol treatment

All the samples were immersed into 75% alcohol solution for 30 min and left until air dry. The samples were subsequently tested and followed with a new treatment cycle.

Chlorine-based solution treatment

All the samples were uniformly sprayed with 1 ml domestic chlorine-based solution (containing 2% NaClO) and left to air dry. The samples were subsequently tested and followed with a new treatment cycle.

UVGI

All the samples were placed into a Sterilization Cabinet, with a 254 nm, 8 W UV light. The distance between the samples and the UV light was kept at 15 cm. All the samples were irradiated for 30 min and placed for 30 min under ambient conditions, and then put into filtration test and subsequently followed with a new treatment cycle.

Other characterizations

The morphologies of all the samples were studied by the scanning electron microscope (SEM, JSM-6510, Japan) and the transmission electron microscope (TEM, Tecnai G2 S-Twin F20, USA). The surface tensions and relative polar components of TFPNMs were analyzed by an optical contact angle meter (DSA100, KRUSS, Germany) at ambient conditions (temperature: 23-25 °C). The pressure drop across the air filters was recorded by a digital differential pressure gauge (AS510, Smart Sensor, China). PM mass concentration and NaCl aerosol number density were measured by a particle counter (DT-9880M, CEM, China). The static quantity was tested by a electrostatic fieldmeter (FMX-004, SIMCO, Japan). The collection of the filtered viral aerosols was conducted by an All-Glass-Impinger (AGI-30, SKC, USA). The preparation and aerosolization of viral solutions were conducted in a class II Biosafety Cabinet (BHC-1300IIB2, AIRTEC., China). The HeLa cells and Vero cells were cultured in a CO_2 cell culture shelves (SANYO Electric Co., Ltd, Japan) and the corresponding cell morphologies were observed by a light microscope (ECLIPSE Ts2, Nikon Co., Ltd, Japan).
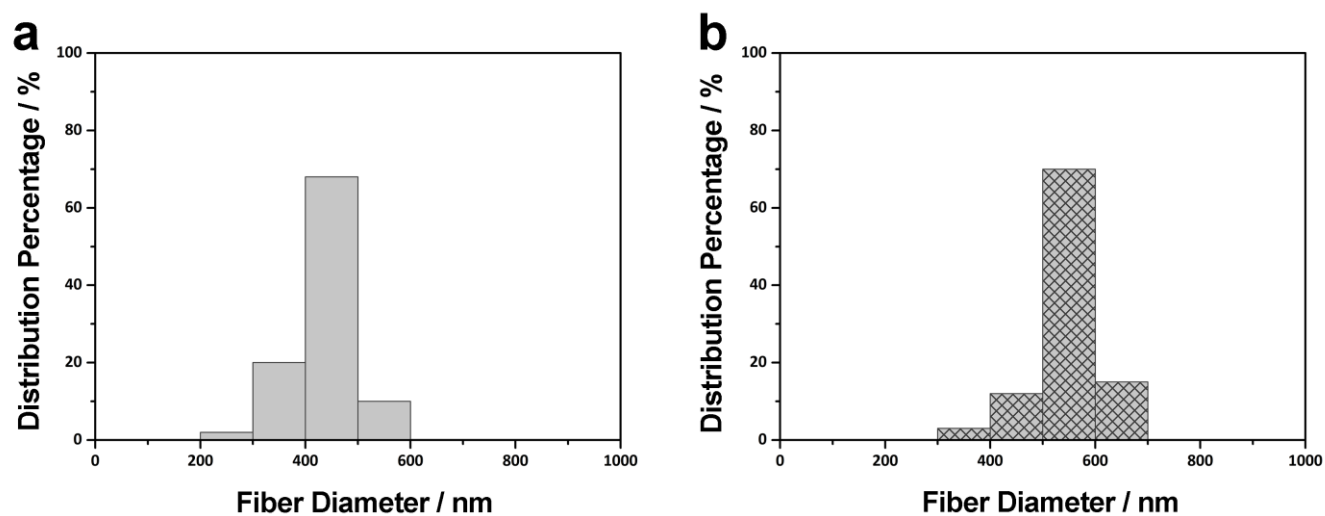
Results and Discussion

Figure S1. Distribution curves of the fiber diameters of a) PAN nanofibers and b) cTFPNs. The PAN fibers had a relatively uniform diameter at around 400-500 nm. After coating, the size of most cTFPNs increased to 500-600 nm.
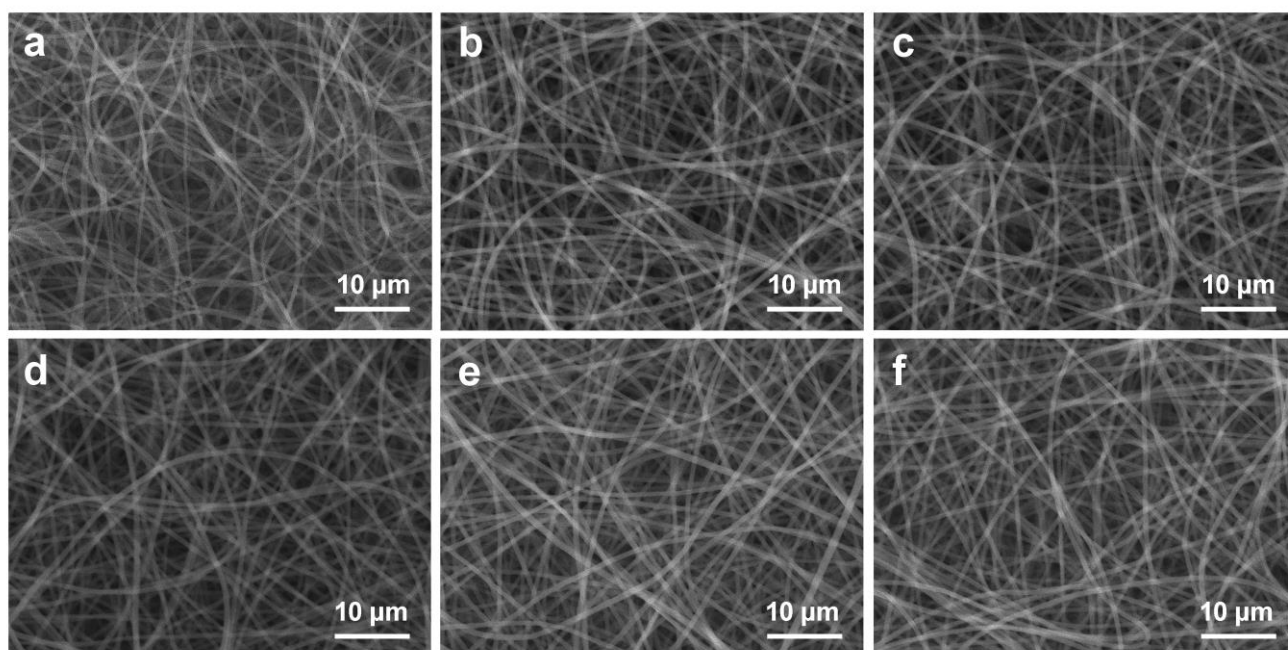

Figure S2. Surface geometries of PAN nanofibers and TFPNs with different terminal groups.
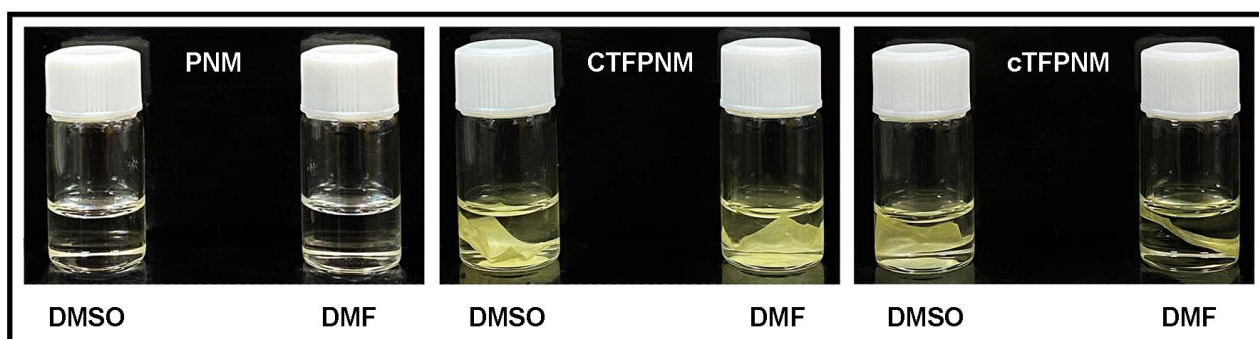a) PAN nanofibers, b) 4-trifluoromethoxy-Ph-terminated TFPNs, c) 4-fluoro-Ph-terminated TFPNs, d) 4-amino-Ph-terminated TFPNs, e) 4- carboxyl-Ph-terminated TFPNs and f) 4-cyan-Ph-terminated TFPFNs. The similar surface geometries with uniform fiber diameters suggest that there is no change occurred during the modification process.

a Before soaking
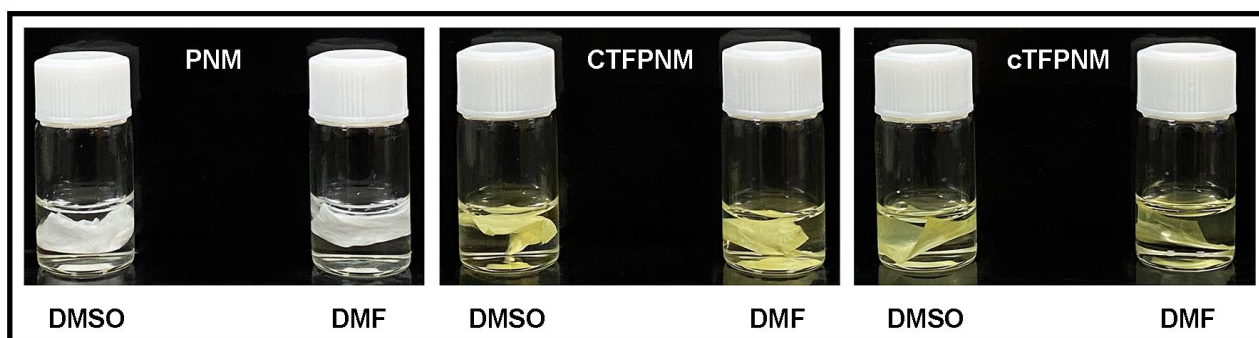
b After soaking

Figure S3. Stability test of TFPNMs in aprotic solvents. Stability of PNM and TFPNMs in dimethylformamide (DMSO, left bottle in all images) and dimethyl sulfoxide (DMF, right bottle in all images). The PNM was completely dissolved in both DMSO and DMF solutions within 5 min. However, the TF layer enhanced the stability of TFPNMs in the aprotic solvents, and the TFPNMs remained stable after soaking for 90 days.
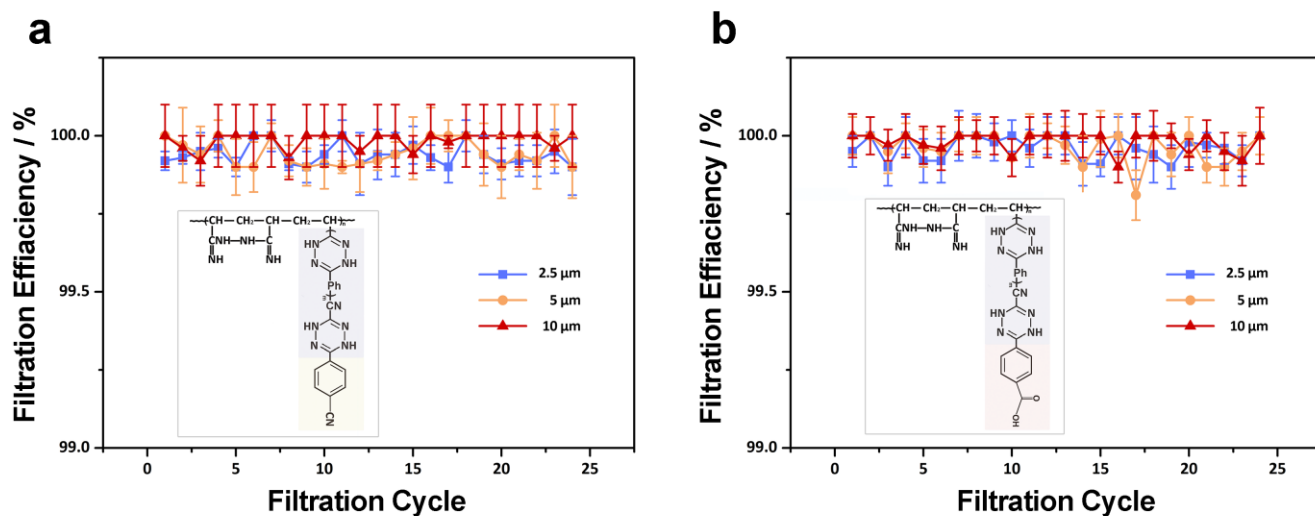
Figure S4. PMs capture capabilities over TFPNMs.
A 24 h evolution of filtration characteristics of a) CTFPNM and b) cTFPNM for $PM_{10-2.5}$ at room temperature. Both highly polar TFPNMs showed FEs of $PM_{10-2.5}$ over 99.90 %.
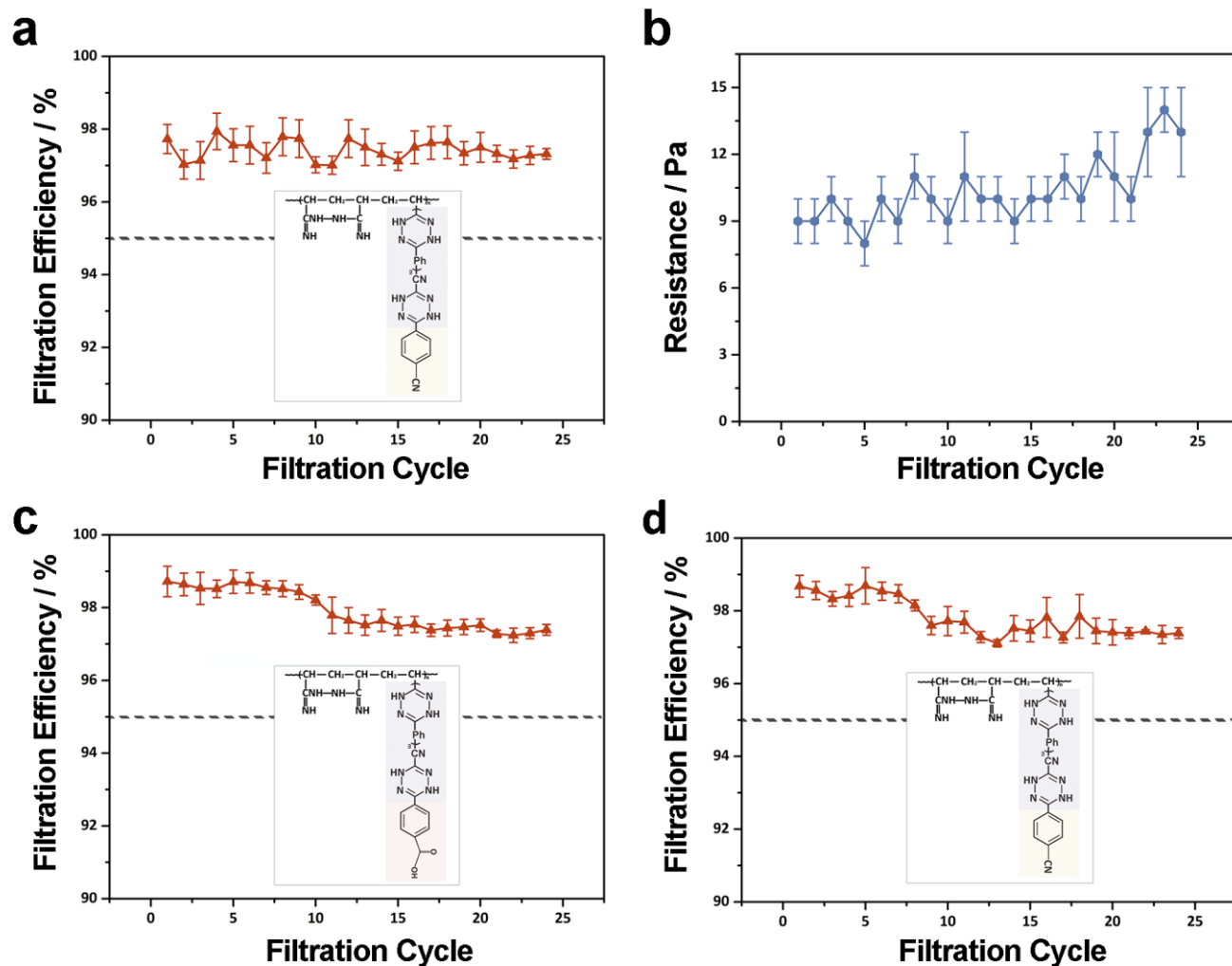
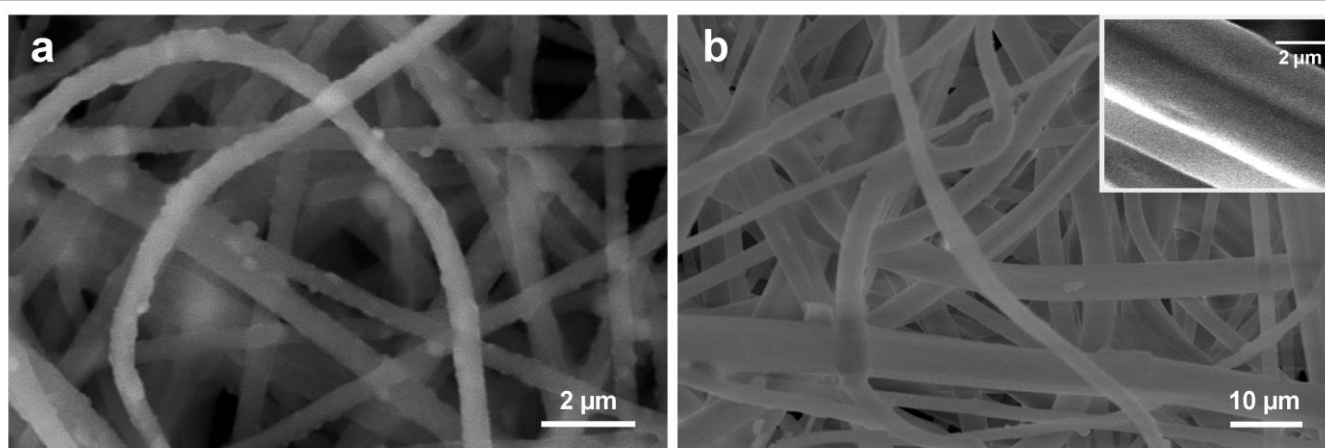**Figure S5. Overall filtration performance of TFPNMs.**
A 24 h evolution of CTFPNM's filtration characteristics at room temperature, a) filtration efficiencies and b) pressure drop. A 24 h evolution of charged TFPNMs' filtration efficiencies at room temperature, including c) charged cTFPNM and d) charged CTFPNM.

Figure S6. Virus capture capability over a) cTFPNM and b) MEO-brand N95 FFR. After 24 h filtering of CV-B4 viral aerosols, the cTFPNM had superior virus capture capability, fine particulates with sizes below 100 nm could be effectively captured. However, for the MEO-brand N95 FFRs, it could be barely observed teeny particulates on the PP fibers after 24 h filtering.
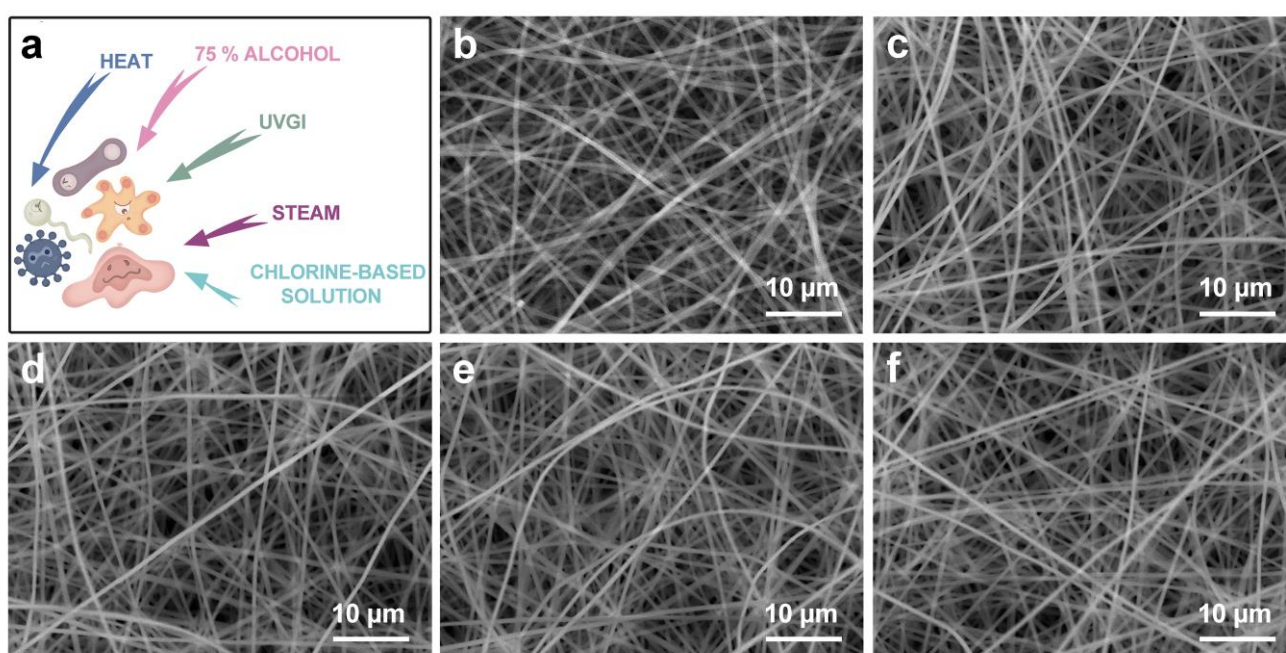
Figure S7. A 10-recycle evolution of cTFPNM characteristic upon various disinfection treatments.
a) The surface geometries of cTFPNMs upon various disinfection treatments are similar to that of the initial membrane, including b) heat treatment, c) steam treatment, d) 75% alcohol treatment, e) chlorine-based solution treatment and f) UVGI treatment. The pressure drops of cTFPNM could be maintained at 9-10 Pa, which also indicates the unchanged surface geometry.
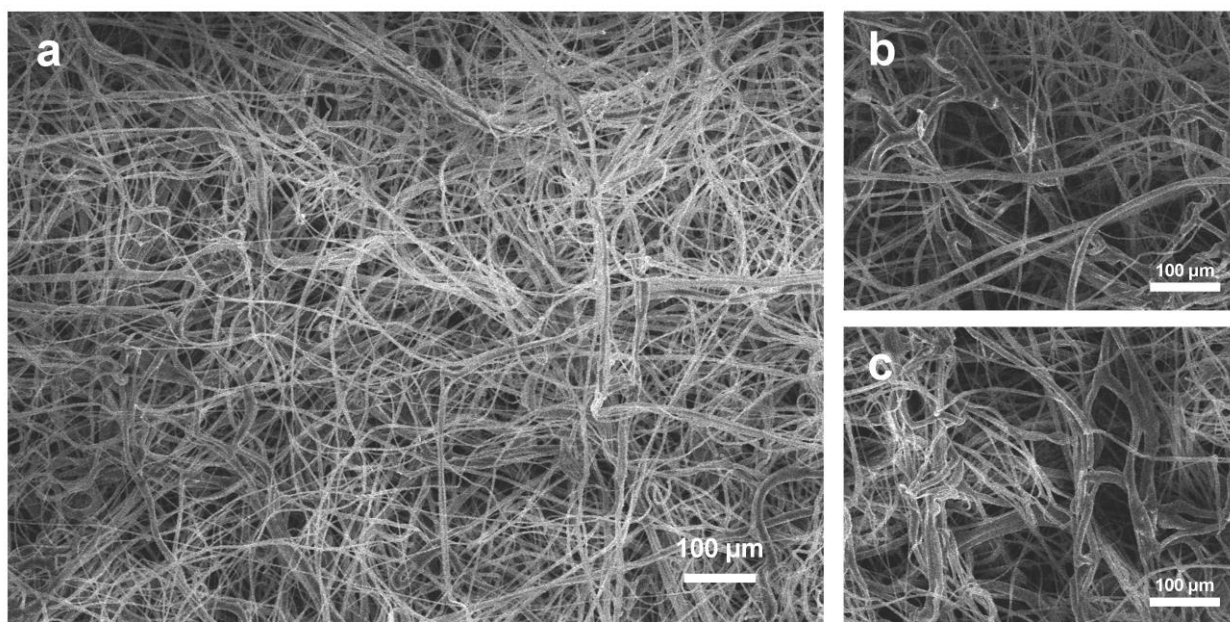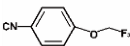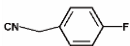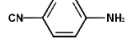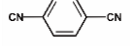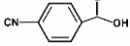
Figure S8. Changes on the geometry of the MEO-brand N95 FFR upon solution-based disinfection treatments.
A slight difference on the surface geometry could be observed between a) the initial MEO-brand N95 FFR and b) the alcohol treated, c) chlorine-based solution treated MEO-brand N95 FFRs. More large void spaces could be observed after the solution-based disinfection treatments, further resulting in the substantial degradation on FEs. The pressure drops of the solution-based methods treated FFRs also changed from 8 Pa to 10 Pa and 5 Pa.

SUPPORTING INFORMATION

Table S1. The surface tension of TFPNMs estimated by OWRK method.

TFPNMs	Molecular Formula of Terminal Groups	γ_S (mJ/m^2) [a]	γ_S^p (mJ/m^2) [b]
4-Trifluoromethoxy-Ph-TFPNM		22.45	2.99
4-Fluoro-Ph-TFPNM		25.61	5.85
4-Amino-Ph-TFPNM		36.07	21.53
4-Cyan-Ph-TFPNM		42.26	31.96
4-Carboxyl-Ph-TFPNM		72.66	66.09

Five liquids were used to increase the accuracy of the estimated results about surface tensions: water, ethylene glycol, dimethylformamide, nitromethane and formamide.

[a] γ_S represents the estimated result about the surface tension of an appointed TFPNM.

[b] γ_S^p represents the estimated result about the polar component of surface tension of an appointed TFPNM.

Table S2. Surface Polarity and Stability of TFPNMs.

TFPNMs	Initial TFPNMs		Disinfected TFPNMs	
	γ_S (mJ/m^2) [a]	γ_S^p (mJ/m^2) [b]	γ_S (mJ/m^2) [a]	γ_S^p (mJ/m^2) [a]
4-Trifluoromethoxy-Ph-TFPNM	22.45	2.99	22.96	2.20
4-Fluoro-Ph-TFPNM	25.61	5.85	26.05	5.92
4-Amino-Ph-TFPNM	36.07	21.53	35.15	22.15
4-Cyan-Ph-TFPNM	42.26	31.96	42.84	32.04
4-Carboxyl-Ph-TFPNM	72.66	66.09	72.72	66.29

The data from all the samples represent the mean and standard deviation of 10 samples. The disinfected TFPNMs were displayed by five different disinfection treatments by the following order: 80 °C heat, steam, 75% alcohol, chlorine-based disinfecting water, UVGI.

[a] γ_S represents the estimated result about the surface tension of an appointed TFPNM.

[b] γ_S^p represents the estimated result about the polar component of surface tension of an appointed TFPNM.

SUPPORTING INFORMATION

Table S3. Overall Filtration Performance of Different Respirator Membranes.

Samples	First Filtration Cycle			After 10 Filtration Cycles			After 24 Filtration Cycles		
	Filtration Efficiency (%)	Pressure Drop (Pa)	QF (Pa^{-1})	Filtration Efficiency (%)	Pressure Drop (Pa)	QF (Pa^{-1})	Filtration Efficiency (%)	Pressure Drop (Pa)	QF (Pa^{-1})
cTFPNM	97.75	9	0.42	97.72	11	0.34	97.42	13	0.28
CTFPNM	97.73	9	0.42	97.68	11	0.34	97.39	13	0.28
Dräger	96.31	14	0.24	95.17	18	0.16	94.67	25	0.11
MEO	96.37	8	0.41	95.95	12	0.26	94.84	15	0.19
KINLEED	95.25	14	0.22	94.66	17	0.17	92.66	24	0.10
3Q	96.25	15	0.22	95.33	18	0.17	94.89	25	0.12
3M	96.42	32	0.10	95.05	38	0.08	93.94	46	0.06

The data from the samples characterized with a flow rate of 5 L/min and NaCl aerosols represent the mean and standard deviation of 10 samples. All the data are related to the initial filtration characteristics and the corresponding characteristics after 10 and 24 filtration cycles, respectively.

Table S4. Disinfection Treatments over cTFPNMs.

Treatment	Treatment Mode	Treatment Time (min)	Filtration Efficiency (%)	Pressure Drop (ΔP/Pa)
Initial Sample			97.73±0.25	10.0±1.0
Dry Heat (80 °C)	Heat Oven	30	97.65±0.22	9.0±1.0
Steam	Boiling Water	10	97.42±0.26	9.0±1.0
Alcohol (75 %)	Immersion	30 (Until Air Dry)	97.45±0.44	10.0±1.0
Chlorine-based Solution (2 %)	Spray and Immersion	10 (Until Air Dry)	97.56±0.48	11.0±1.0
UVGI (254 nm, 8 W)	Sterilization Cabinet	30	97.33±0.13	9.0±1.0

The data from the samples displayed upon five different disinfection treatments represent the mean and standard deviation of 10 samples.

Table S5. Influence on filtration efficiency of multiple N95 FFRs upon various disinfection treatments after first cycle.

Treatments	Filtration Efficiency (%)				
	Dräger	MEO	KINLEED	3Q	3M
Initial Sample (Corona Charged)	96.31±0.25	96.37±0.2	95.25±0.3	96.25±0.22	96.42±0.4
Dry Heat (80 °C)	96.20±0.18	96.30±0.26	95.45±0.30	96.41±0.35	96.35±0.28
Steam	95.41±0.30	95.32±0.25	94.41±0.20	95.32±0.22	92.94±0.20
Ethanol (75 %)	78.95±0.55	68.58±0.55	77.26±0.25	76.03±0.15	73.35±0.35
Chlorine-based (2 %)	69.10±0.15	57.33±0.24	87.15±0.23	71.21±0.25	76.02±0.10
UVGI (254 nm, 8 W)	93.82±0.65	96.28±0.25	95.41±0.35	96.60±0.60	96.54±0.48

The data from the samples displayed upon five different disinfection treatments represent the mean and standard deviation of 10 samples.

Table S6. Influence on pressure drop of multiple N95 FFRs upon various disinfection treatments after first cycle.

Treatments	Pressure Drop (Pa)				
	Dräger	MEO	KINLEED	3Q	3M
Initial Sample (Corona Charged)	14±1	8±1	14±1	15±1	32±1
Dry Heat (80 °C)	13±2	9±1	15±2	15±1	34±2
Steam	14±1	8±1	15±1	13±1	37±2
Ethanol (75 %)	14±2	10±1	12±1	14±1	34±2
Chlorine-based (2 %)	9±1	5±1	16±1	12±1	37±2
UVGI (254 nm, 8 W)	16±2	6±1	13±2	15±2	35±2

The data from the samples displayed upon five different disinfection treatments represent the mean and standard deviation of 10 samples.

SUPPORTING INFORMATION

Note S1. Estimation of the Surface Tension of TFPNMs

The surface tension of the TFPNMs was estimated by the OWRK method (Owen, Wendt, Rabel and Kael).[6] It simply depends on the contact angle of two different kinds of liquids, which can estimate the surface tension of solids and develop the corresponding dispersion and polar interfacial attractions.

Work of adhesion on the interface of solid surface and liquid can be divided into two parts: polar and dispersion. As suggested by Fowkes, the attractive forces at solid surface can be contributed by the polar and dispersive interfacial attractions, and the polar-dispersive interactions can be negligible.

$$W_a = \gamma_S + \gamma_L - \gamma_{SL} \qquad \text{eq. S1}$$

$$W_a = W_a^d + W_a^p = 2\left(\sqrt{\gamma_S^d \gamma_L^d} + \sqrt{\gamma_S^p \gamma_L^p}\right) \qquad \text{eq. S2}$$

In particular, the equation S2 could be combined with equation S1 based on the Young's equation (eq. S3), when contact angel θ > 0,

$$\cos\theta = \frac{\gamma_S - \gamma_{SL}}{\gamma_L} \qquad \text{eq. S3}$$

By further concise equations with measurable quantities, we have,[7]

$$z \frac{\gamma_L(1+\cos\theta)}{2\sqrt{\gamma_L^d}} = \sqrt{\gamma_S^d} + \sqrt{\gamma_S^p} \frac{\sqrt{\gamma_L^p}}{\sqrt{\gamma_L^d}} \qquad \text{eq. S4}$$

In the OWRK method, γ_S^d and γ_S^p can be estimated with two liquids or more, for example, water (γ_L^d = 21.8 mJ/m^2, γ_L^p = 51.0 mJ/m^2) and formamide (γ_L^d = 39.5 mJ/m^2, γ_L^p = 18.7 mJ/m^2).

When the calculated results fulfill the above eq. S4, the γ_S^d and γ_S^p of different solid surfaces could be estimated. In our work, five liquids are used to increase the accuracy of the estimated results about surface tensions: water, ethylene glycol, dimethylformamide, nitromethane and formamide.

In the above note, the W_a refers to the work of adhesion, W_a^d and W_a^p are the dispersion and polar components of W_a. γ_S and γ_L are the solid and liquid surface tension, respectively, and the γ_{SL} is the interfacial tension. γ_S^d and γ_L^d represent the dispersion component of γ_S and γ_L. γ_S^p and γ_L^p represent the polar component of γ_S and γ_L. θ refers to the specific liquid-solid contact angle.

References

[1]   Q. Wang, Y. Wang, B. Wang, Z. Liang, J. Di, J. Yu, *Chem. Sci.* **2019**, *10*, 6382-6389.

[2]   T. C. Lin, G. Krishnaswamy, D. S. Chi, *Clin. Mol. Allergy* **2008**, *6*, 3.

[3]   N. Turgeon, M. J. Toulouse, B. Martel, S. Moineau, C. Duchaine, *Appl. Environ. Microbiol.* **2014**, *80*, 4242-4250.

[4]   C. M. Carthy, D. J. Granville, K. A. Watson, D. R. Anderson, J. E. Wilson, D. Yang, D. W. C. Hunt, B. M. McManus, *J. Virol.* **1998**, *72*, 7669-7675.

[5]   a) G. Kärber, *Arch. Exp. Path. Pharmacol.* **1931**, *162*, 480-483; b) C. Lei, J. Yang, J. Hu, X. Sun, *Virol. Sin.* **2021**, *36*, 141-144.

[6]   a) D. K. Owens, R. C. Wendt, *J. Appl. Polym. Sci.* **1969**, *13*, 1741–1747; b) D. H. Kaelble, *J. Adhes.* **2008**, *2*, 66-81.

[7]   Y. Wang, J. Di, L. Wang, X. Li, N. Wang, B. Wang, Y. Tian, L. Jiang, J. Yu, *Nat. Commun.* **2017**, *8*, 575.

Author Contributions

J.H.Y. conceived and designed the project. Q.F.W. carried out the overall performance experiments and related analysis. Y.Z.W. and W.B.L. helped with the filtration characteristic experiments and the pressure drop analysis. J.C.D. participated in some discussion. G.Q.W. conducted the cytopathic effect and virus titration tests, Q.F.W., X.Z.L and X.Y.Z. carried out the relative experiments to evaluate the virus filtration characteristics. Q.F.W. wrote the manuscript, and J.H.Y. revised the manuscript.